AIAA JOURNAL
Vol. 46, No. 11, November 2008

Nonlinear Response Structural Optimization of a Joined Wing Using Equivalent Loads

Y. I. Kim* and G. J. Park†
Hanyang University, Ansan City, 426-791, Republic of Korea
R. M. Kolonay‡ and M. Blair§
U.S. Air Force Research Laboratory, Wright–Patterson Air Force Base, Ohio 45433
and
R. A. Canfield¶
U.S. Air Force Institute of Technology,
Wright–Patterson Air Force Base, Ohio 45433-7765

DOI: 10.2514/1.33428

The joined wing is a new concept of the airplane wing. The forewing and the aft wing are joined together in the joined wing. The joined wing can lead to increased aerodynamic performances and reduction of the structural weight. The structural behavior of the joined wing has a high geometric nonlinearity according to the external loads. Therefore, the nonlinear behavior should be considered in the optimization of the joined wing. It is well known that conventional nonlinear response optimization is extremely expensive; thus, the conventional method is almost impossible to use for large-scale structures such as the joined wing. In this research, geometric nonlinear response optimization of a joined wing is carried out by using equivalent loads. The used structure is a joined wing that is currently being developed in the U.S. Air Force Research Laboratory. Equivalent loads are the load sets that generate the same response field in linear analysis as that from nonlinear analysis. In the equivalent loads method, the external loads are transformed to the equivalent loads for linear static analysis, and linear response optimization is carried out based on the equivalent loads. The design is updated by the results of linear response optimization. Nonlinear analysis is carried out again and the process proceeds in a cyclic manner until the convergence criteria are satisfied. It was verified that the equivalent loads method is equivalent to a gradient-based method; therefore, the solution is the same as that of exact nonlinear response optimization. The fully stressed design method is also used for nonlinear response optimization of a joined wing. The results from the fully stressed design and the equivalent loads method are compared.

I. Introduction

THE joined-wing airplane may be defined as an airplane that incorporates tandem wings arranged to form diamond shapes in both top and front views. Figure 1 shows a general joined-wing aircraft in which the forewing and aft wing are joined. Wolkovich [1] published the joined-wing concept in 1986. The joined wing has the advantage of a longer range and loiter than those of a conventional wing. Generally, the weight of the joined-wing aircraft is lighter than that of a conventional wing. Miura et al. [2] employed an optimization method to study the effects of joined-wing geometry parameters on structural weight. Gallman and Kroo [3] offered many recommendations for the design methodology of a joined wing. They used the fully stressed design (FSD) for optimization. Blair et al. [4] initiated nonlinear exploration on a joined-wing configuration in 2005. The U.S. Air Force Research Laboratory (AFRL) has been developing an airplane with the joined wing to complete a long-endurance surveillance mission [4–8]. Lee et al. [9] performed dynamic response structural optimization of a joined wing using equivalent static loads. They considered the dynamic effect of the joined wing in optimization.

The joined wing has high geometric nonlinearity [4]. Geometric nonlinearity should be considered when deformation is large enough so that the equilibrium equations must be written with respect to the deformed structural geometry. Also, the loads may change directions as they increase [10]. Generally, the applied loads act vertically as a lifting force for the joined wing. The displacement of the wing tip becomes very large as the applied loads increase. The load directions are changed due to the large deformation of the joined wing. Therefore, the followed force, at the last stage of the deformation, should be considered.

Gust is the movement of the air in turbulence, and the gust load has a large impact on the airplane [11]. The gust loads are the most important loading conditions when an airplane wing is designed. The gust loads for a joined wing have been calculated by the researchers of the AFRL [4]. Static loads for the gust can be generated from an aeroelastic model by the panel method [12].

During the past decades, many finite element theories considering nonlinearity have been developed and applied to practical problems [10,13,14]. However, it is not easy to mathematically optimize a structure with nonlinear behavior, because calculation of nonlinear sensitivity is extremely difficult or expensive [15–17]. Sensitivity information is used to make the decision of the direction of the design change [18–20]. In a nonlinear system, a linear relationship between the external force and structural behavior cannot be expected. Therefore, many nonlinear analyses are required in the optimization process.

In previous research, Blair et al. [4] performed nonlinear structural optimization of a joined wing using FSD. FSD is a non-gradient-based algorithm that is used for resizing element thicknesses or areas so as to produce a design in which each designed property is subject to its maximum allowable stress. FSD provides a rapid means of

Received 13 July 2007; revision received 24 May 2008; accepted for publication 9 June 2008.

*Graduate Student, Department of Mechanical Engineering.
†Professor, Department of Mechanical Engineering; gjpark@hanyang.ac.kr. Senior Member AIAA (Corresponding Author).
‡Aerospace Engineer, Air Vehicles Directorate. Member AIAA.
§Aerospace Engineer, Air Vehicles Directorate. Associate Fellow AIAA.
¶Associate Professor, Department of Aeronautics and Astronautics. Associate Fellow AIAA.

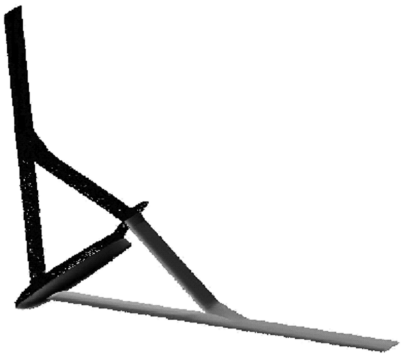

Fig. 1 Joined-wing configuration.

performing initial sizing of aerospace vehicles and allows for the design of a virtually unlimited number of element sizes. The FSD method is efficient for designing structures subject only to stress constraints. The thickness or area can be used as design variables. The solution of FSD is not relatively as exact as that of the gradient-based optimization method [18,21].

A modified gradient-based optimization algorithm has been proposed for nonlinear response structural optimization. This algorithm is called nonlinear response optimization using equivalent loads (NROEL) [22–24]. A nonlinear response optimization problem is converted to linear response optimization with equivalent loads. The original loads are changed to a set of equivalent loads based on the responses. The set of loads are used as multiple loading conditions of linear response optimization. The design is changed in linear response optimization. A new set of equivalent loads is made again by using nonlinear analysis and the process proceeds in a cyclic fashion until the convergence criteria are satisfied. Only basic theories have been defined in the previous research. In this research, the theory is applied to a large-scale optimization problem of a joined wing. Also, the treatment of stress constraints is improved.

A finite element model for a joined wing is established. Nonlinear finite element analysis is performed by considering geometric nonlinearity. As mentioned earlier, gust loads are critical for the design of the joined wing; therefore, the followed forces of the gusts are considered in the analysis. Structural optimization is performed to incorporate the results of nonlinear analysis. The NROEL method is employed for nonlinear response structural optimization. Size optimization for the thickness of each finite element is conducted to reduce the structural mass while design conditions are satisfied. ABAQUS is used for nonlinear analysis and GENESIS is used for the linear response optimization process in NROEL [25,26]. Computer programs have been developed to apply the NROEL method.

II. Nonlinear Structural Optimization Using Equivalent Loads

There are several methods for nonlinear structural optimization. The conventional gradient-based method gives an excellent solution. [18–20]. However, because the method is extremely expensive due to sensitivity analysis, it is not applicable to large-scale problems. The FSD method and the response surface method (RSM) are non-gradient-based optimization algorithms [17,18]. The solution of these methods is not as exact as that of the gradient-based optimization method. Moreover, the RSM method cannot solve a large-scale problem that has several hundreds of design variables. The NROEL method is a gradient-based optimization algorithm and the joined-wing structure is optimized by NROEL in this research. The method is explained as follows:

A. Calculation of Equivalent Loads

The equivalent loads (ELs) are defined as the loads for linear analysis, which generate the same response fields as those of nonlinear analysis. According to the finite element method [10,13,14], the equilibrium equation of a structure with nonlinearity is

$$\mathbf{K}_N(\mathbf{b}, \mathbf{z}_N)\mathbf{z}_N = \mathbf{f} \tag{1}$$

where $\mathbf{K}$ is the stiffness matrix that is the function of the design variable vector $\mathbf{b}$ and the nodal displacement vector $\mathbf{z}$, the subscript N means that the displacement is obtained by nonlinear analysis, $\mathbf{f}$ is the external load vector, and $\mathbf{z}_N$ is obtained from Eq. (1). The equivalent load for displacements is defined as

$$\mathbf{f}^{\mathbf{z}}_{\text{eq}} = \mathbf{K}_L(\mathbf{b})\mathbf{z}_N \tag{2}$$

where $\mathbf{f}^{\mathbf{z}}_{\text{eq}}$ is the equivalent load vector for displacement, $\mathbf{K}_L$ is the linear stiffness matrix, $\mathbf{z}_N$ is the nodal displacement vector from Eq. (1); $\mathbf{f}^{\mathbf{z}}_{\text{eq}}$ is used in Eq. (3), which is the equation of linear analysis using the finite element method as follows:

$$\mathbf{K}_L(\mathbf{b})\mathbf{z}_L = \mathbf{f}^{\mathbf{z}}_{\text{eq}} \tag{3}$$

where the nodal displacement vector $\mathbf{z}_L$ has the same values as the nonlinear nodal displacement vector $\mathbf{z}_N$ in Eq. (1). Therefore, if the equivalent load $\mathbf{f}^{\mathbf{z}}_{\text{eq}}$ is used as an external load in linear response optimization, the same displacements as the nonlinear response can be considered throughout linear response optimization. Figure 2 shows this process.

Although the load $\mathbf{f}^{\mathbf{z}}_{\text{eq}}$ can generate the same displacements as the nonlinear displacements, it does not generate the same stress responses because the relationships between the strain and displacement, as well as the strain and stress, have nonlinearity. Thus, the equivalent loads for the stresses should be separately calculated. Mathematically, the equivalent loads are calculated by multiplying the linear stiffness matrix and the displacement vector. However, the stress response vector cannot be calculated directly from the stiffness matrix. Therefore, we need an additional procedure.

The stress response $\boldsymbol{\sigma}_N$ is obtained from Eq. (1) of nonlinear analysis. The obtained stress is used as the initial stress. Therefore, the equivalent load for stresses is calculated as follows:

$$\mathbf{K}_L(\mathbf{b})\mathbf{z}^{\boldsymbol{\sigma}}_L = -\bar{\mathbf{f}}_I(\boldsymbol{\sigma}_N) \tag{4}$$

$$\mathbf{f}^{\boldsymbol{\sigma}}_{\text{eq}} = \mathbf{K}_L(\mathbf{b})\mathbf{z}^{\boldsymbol{\sigma}}_L \tag{5}$$

where $\mathbf{f}^{\boldsymbol{\sigma}}_{\text{eq}}$ is the equivalent load vector for the stress response, $\mathbf{K}_L$ is the linear stiffness matrix, and $\boldsymbol{\sigma}_N$ from Eq. (1) is used as the initial stress effect $-\bar{\mathbf{f}}_I(\boldsymbol{\sigma}_N)$ in Eq. (4) of linear analysis. Equation (4) is linear static initial stress analysis, where $\boldsymbol{\sigma}_N$ is used as input. Equation (4) is used to calculate the displacement vector $\mathbf{z}^{\boldsymbol{\sigma}}_L$. The superscript $\boldsymbol{\sigma}$ means the displacement for the calculation of the equivalent loads concerning the stress response, and $\mathbf{f}^{\boldsymbol{\sigma}}_{\text{eq}}$ can be calculated by multiplying $\mathbf{K}_L$ and $\mathbf{z}^{\boldsymbol{\sigma}}_L$ as shown in Eq. (5).

The calculated force vector $\mathbf{f}^{\boldsymbol{\sigma}}_{\text{eq}}$ can be used as follows:

$$\mathbf{K}_L(\mathbf{b})\mathbf{z}_L = \mathbf{f}^{\boldsymbol{\sigma}}_{\text{eq}} \tag{6}$$

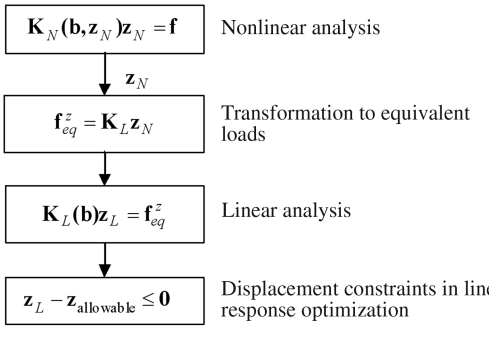

Fig. 2 Generation of equivalent loads for displacement constraints.

where $\mathbf{z}_L$ is an unknown vector. The stress response $\boldsymbol{\sigma}_L$ is obtained from Eq. (6) of linear analysis. However, this stress response may not be exactly the same as that from nonlinear analysis, because the integral points for calculation of stresses are different in nonlinear static analysis and initial stress analysis. The difference can be adjusted to $\hat{\boldsymbol{\sigma}}_L$ as follows:

$$\alpha_i = \frac{\sigma_{Ni}}{\sigma_{Li}} \tag{7a}$$

$$\hat{\sigma}^{\,j}_{Li} = \sigma^j_{Li} \cdot \alpha_i \tag{7b}$$

where α is the stress correction factor, i is the element number, σ_{Ni} is the nonlinear stress response from Eq. (1), and σ_{Li} is the linear stress response from Eq. (6). The stress correction factor is calculated from Eq. (7a).

In Eq. (7b), the superscript j means the iteration number in linear response optimization. The corrected stress $\hat{\sigma}^j_{Li}$ is calculated from Eq. (7b). When j is equal to zero, the corrected stress is exactly equivalent to the stress response σ_{Ni} in nonlinear static analysis with the initial design. The stress response σ^j_{Li} is changed while the design is changed in linear response optimization. Because the correction factor α and the equivalent loads $\mathbf{f}^{\sigma}_{\text{eq}}$ are constant in linear response optimization, the corrected stress $\hat{\sigma}^j_{Li}$ is changed as the design variables change. If the equivalent load $\mathbf{f}^{\sigma}_{\text{eq}}$ is used as an external load and the stress correction factor α is applied in linear static optimization, the same stress as the nonlinear stress can be considered in the linear static response optimization process. Figure 3 presents this process.

If the problem has a displacement constraint as well as a stress constraint, equivalent loads should be calculated with respect to each response, and the sets of the equivalent loads are used in linear response optimization as multiple loading conditions.

B. Steps for NROEL

The overall process of the NROEL algorithm is illustrated in Fig. 4. The steps of the algorithm are as follows:

1) Set initial values and parameters (design variables are $\mathbf{b}^{(k)} = \mathbf{b}^{(0)}$, cycle number $k = 0$, and the convergence parameter is a small number ε).

2) Perform nonlinear analysis with $\mathbf{b}^{(k)}$. Hence, the linear stiffness matrix and nonlinear responses are obtained.

3) Calculate the equivalent load sets as follows:

$$\mathbf{f}^{\,z,(k)}_{\text{eq}} = \mathbf{K}_L(\mathbf{b})\mathbf{z}_N \quad \text{and} \quad \mathbf{f}^{\sigma,(k)}_{\text{eq}} = \mathbf{K}_L(\mathbf{b})\mathbf{z}^{\sigma}_L \tag{8}$$

4) When $k = 0$, go to step 5. When $k > 0$, if

$$\|\mathbf{b}^{(k)} - \mathbf{b}^{(k-1)}\| \le \varepsilon \tag{9}$$

then terminate the process. Otherwise, go to step 5.

5) Solve the following linear static response optimization problem:

Find $\mathbf{b}^{(k+1)}$.

To minimize $f(\mathbf{b}^{(k+1)})$.

Subject to

$$\mathbf{K}_L(\mathbf{b}^{(k+1)})\mathbf{z} - \mathbf{f}^{\mathbf{z},(k)}_{\text{eq}} = 0$$
$$\mathbf{K}_L(\mathbf{b}^{(k+1)})\mathbf{z} - \mathbf{f}^{\boldsymbol{\sigma},(k)}_{\text{eq}} = 0$$
$$g_j(\mathbf{b}^{(k+1)}, \mathbf{z}, \hat{\boldsymbol{\sigma}}) \le 0 \quad (j = 1, \ldots, m)$$
$$\mathbf{b}^{(k+1)}_{iL} \le \mathbf{b}^{(k+1)}_i \le \mathbf{b}^{(k+1)}_{iU} \quad (i = 1, \ldots, n)$$

The external load $\mathbf{f}_{\text{eq}}$ is the equivalent load vector. The two equivalent load sets are used as multiple loading conditions during the optimization process.

6) Update the design results, set $k = k + 1$, and go to step 2.

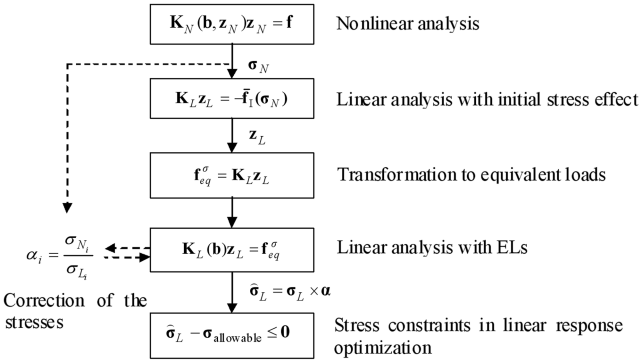

Fig. 3 Generation of equivalent loads for stress constraints.

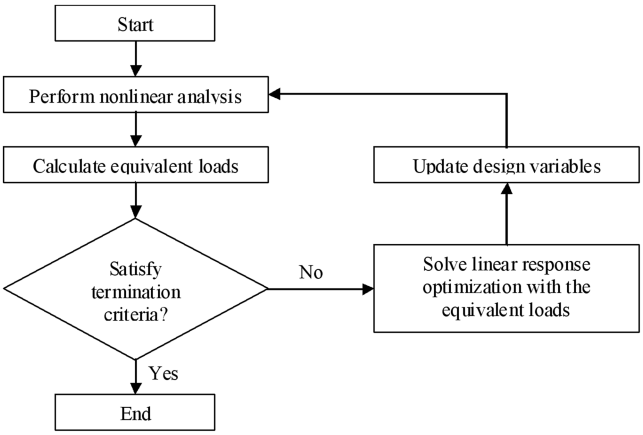

Fig. 4 Optimization process using the equivalent static loads.

III. Analysis of the Joined Wing

A. Finite Element Modeling of the Joined Wing

The joined wing consists of five parts, which are the forewing, the aft wing, the midwing, the tip wing, and the edge around the joined wing. The parts are illustrated in Fig. 5. Each part is composed of the top skin, the bottom skin, the spar, and the rib. The length from the wing tip to the wing root is 38 m, and the length of the chord is 2.5 m. The model has 3027 elements with 2857 quadratic elements, 156 triangular elements, and 14 rigid elements. Rigid elements make connections between the nodes of the aft-wing root and the center node of the aft-wing root. The structure has two kinds of aluminum materials. One has Young's modulus of 72.4 GPa, the shear modulus of 27.6 GPa, and the density 2770 kg/m^3. The other has 36.2 GPa, 13.8 GPa, and 2770 kg/m^3, respectively. The latter material is only used for elements of the edge part. The former material is used for the entire elements except for the edge part [4].

B. Loading Conditions of the Joined Wing

Eleven loading conditions for structural optimization have been defined by the AFRL [4]. These loading conditions are composed of

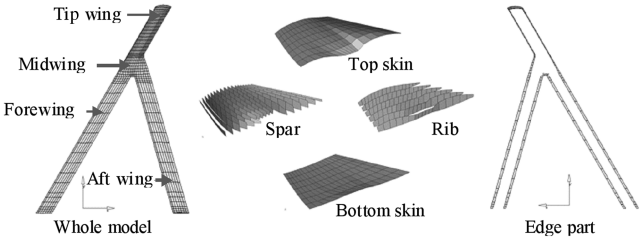

Fig. 5 Finite element modeling of the joined wing.

Table 1 Load data of the joined wing

Number of loading condition	Load type	Mission leg
1	2.5 g pullup	Ingress
2	2.5 g pullup	Ingress
3	2.5 g pullup	Loiter
4	2.5 g pullup	Loiter
5	2.5 g pullup	Egress
6	2.5 g pullup	Egress
7	2.5 g pullup	Egress
8	Gust (maneuver)	Descent
9	Gust (cruise)	Descent
10	Taxi (1.75 g impact)	Takeoff
11	Impact (3.0 g landing)	Landing

seven maneuver loads, two gust loads, one takeoff load, and one landing load, as shown in Table 1. Each loading condition has a different loading direction and magnitude. The gust loading conditions are especially important in these loading conditions. Gust is the movement of the air in turbulence, and the gust load has a large impact on the airplane. Static loads for the gust can be generated from an aeroelastic model that uses the panel method [12]. The panel method is used to calculate the velocity distribution along the surface of the airfoil. Panel methods have been developed to analyze the flowfield around arbitrary bodies in two and three dimensions. The surface of the airfoil is divided into trapezoid panels. Mathematically, each panel induces a velocity on itself. This velocity can be expressed by relatively simple equations that contain geometric relations such as distances and angles between the panels only. The panel method is referred to as a boundary-element method in some publications [12]. When the deformation is large, the direction of an external force is changed according to the deformation. The followed force means the changed force for the deformation. As mentioned earlier, the followed forces at the last state of the deformation are used [4].

Linear and nonlinear response optimizations are performed in this research. All loading conditions are used for linear response optimization, whereas only two gust loading conditions are used for nonlinear response optimization, because the geometric nonlinearity effect of the joined wing largely occurs in the gust loading conditions. A relatively small nonlinear effect occurs in other loading conditions.

C. Boundary Conditions of the Joined Wing

The roots of the forewing and the aft wing are joined to the fuselage. The entire part of the forewing root is attached to the fuselage. Therefore, all the degrees of freedom in six directions are fixed. On the other hand, the aft-wing root can be rotated with respect to the y axis in Fig. 6. The boundary nodes of the aft-wing root are rigidly connected to the center node. The center node has an enforced rotation with respect to the y axis. The boundary nodes are set free in the x and z translational directions. Other degrees of freedom are fixed. The enforced rotation generates torsion on the aft wing and has quite an important aerodynamic effect. The amounts of the enforced rotation are from −0.0897 to 0 rad [4]. These rotational values are different in each mission leg. The boundary conditions are illustrated in Fig. 6.

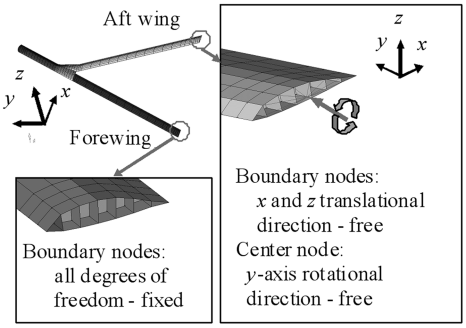

Fig. 6 Boundary conditions of the joined wing.

D. Geometric Nonlinearity of the Joined Wing

Linear and nonlinear analyses are performed under all loading conditions. The design data are adopted from [4] and the data are used for the initial design of the later optimization process. Table 2 shows the results of the analyses. As shown in Table 2, most of the maximum displacements from nonlinear analysis are larger than those of linear analysis. In particular, the difference of the maximum stresses between linear and nonlinear analyses is quite large under the gust loading conditions (loading conditions 8 and 9).

We can see large geometric nonlinearity of the joined wing. Therefore, nonlinear analysis and nonlinear response optimization are required for the joined-wing design. Figure 7 illustrates the deformed shape of the joined wing under the gust loading condition of the cruise speed (loading condition 9). The wing-tip displacement of nonlinear analysis is about 5 times larger than that of linear analysis. Figures 8 and 9 illustrate the stress contours of the joined wing under the cruise-speed gust loading condition. Large stresses occur at the middle spars of the aft wing. The stresses from nonlinear analysis are quite large compared with those from linear analysis. The maximum stress is about 3.21 GPa in nonlinear analysis under the gust loading condition of the cruise speed. This value is very large because the maximum stress of linear analysis under the gust loading condition of the cruise speed is 296.51 MPa. Moreover, it is larger than the allowable stress 179 MPa.

Buckling analysis is performed under all loading conditions. The critical buckling rates for the maneuver gust and cruise-speed gust conditions are 74 and 67% of the gust load, respectively. The buckling primarily occurs at the aft wing. The critical buckling rate of the taxi crater impact load is 108%. The buckling rates of other maneuver loads are 166% and higher. When the buckling rate is more

Table 2 Wing-tip displacements of the linear and nonlinear analyses

	Linear analysis		Geometric nonlinear analysis	
Number of loading condition	Max disp	Max stress	Max disp	Max stress
1	1.52 m	152.03 MPa	1.78 m	135.57 MPa
2	1.45 m	145.10 MPa	1.77 m	143.56 MPa
3	0.79 m	181.03 MPa	1.13 m	171.64 MPa
4	0.67 m	182.85 MPa	1.24 m	204.63 MPa
5	1.84 m	129.41 MPa	2.38 m	195.15 MPa
6	1.09 m	130.72 MPa	1.97 m	249.66 MPa
7	1.06 m	132.47 MPa	2.03 m	275.75 MPa
8 (gust: maneuver)	3.70 m	228.96 MPa	20.56 m	3003.40 MPa
9 (gust: cruise)	4.63 m	296.51 MPa	21.99 m	3205.80 MPa
10	−3.32 m	241.94 MPa	Did not converge	
11	−0.54 m	158.76 MPa	−0.56 m	160.00 MPa

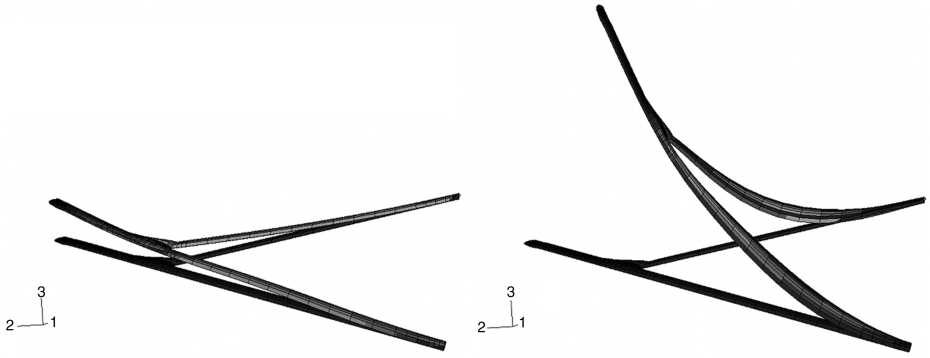

a) Linear analysis b) Nonlinear analysis

Fig. 7 Deformation of the joined wing under the gust loading condition.

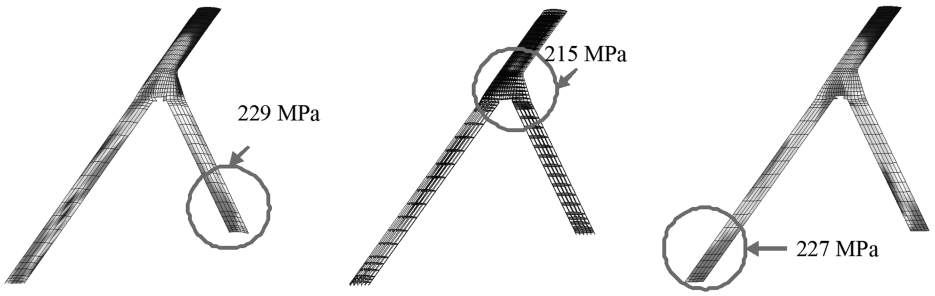

a) Topskin b) Rib and spar c) Bottom skin

Fig. 8 Stress contours from linear analysis of a joined wing.

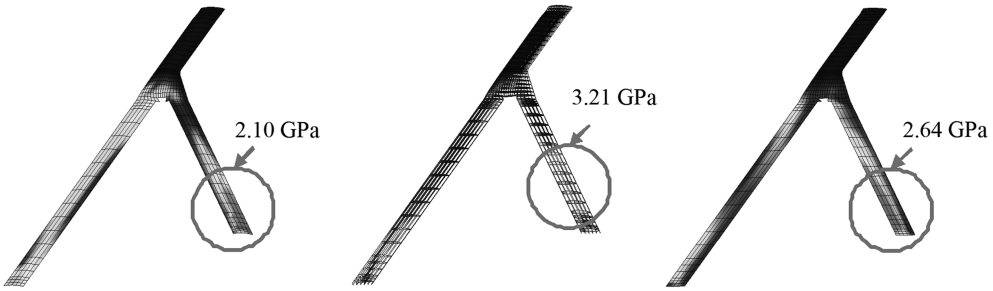

a) Topskin b) Rib and spar c) Bottom skin

Fig. 9 Stress contours from nonlinear analysis of a joined wing.

than 100%, the buckling safety is satisfied. Therefore, the buckling safety is not satisfied by the initial design.

IV. Structural Optimization of the Joined Wing

A. Definition of Design Variables

As mentioned earlier, the finite element method model has 3027 elements. Each element thickness is a design variable. However, the edge part and rigid beams of the aft-wing root are not used as design variables. Therefore, the number of design variables is 2559. The upper and lower bounds are defined for each part: 0.001016, 0.0001277, and 0.000254 m are used as the lower bounds of the skin part, the tip-wing spar part and other wing spars, and the rib part, respectively. The upper bound of the skin part is 0.05 m and the upper bound of the spar and rib parts is 0.08 m.

B. Formulation

The optimization problem is formulated as follows:

Find t_i $(i = 1, \ldots, 2559)$.

To minimize mass.

Subject to

$$|\sigma_j| \leq \sigma_{\text{allowable}} \quad (j = 1, \ldots, 2559)$$

$$0.001016 \text{ m} \leq t_{\text{skin part}} \leq 0.05 \text{ m}$$

$$0.000127 \text{ m} \leq t_{\text{tip wing part}} \leq 0.05 \text{ m}$$

$$0.000254 \text{ m} \leq t_{\text{wing spars and ribs}} \leq 0.08 \text{ m}$$

The mass of the initial model is 3584 kg. First, linear response optimization is carried out for the initial model. Second, the optimum of the linear response optimization is the initial design of nonlinear response optimization. The material of the joined wing is aluminum. The allowable von Mises stress for aluminum is set by 269 MPa. because the safety factor 1.5 is used, the allowable stress is reduced to 179 MPa [4]. Stresses of all the elements except for the edge part should be less than the allowable stress 179 MPa. The buckling constraint is not considered.

C. Programming for the Equivalent Loads Method

In this research, ABAQUS [25] is used for nonlinear response analysis and GENESIS [26] is used for linear response optimization.

Table 3 Results of linear response optimization

Iteration no.	Optimum value, kg	Constraint violation, %
0	3583.5	211.5
1	4267.8	94.3
2	4883.9	28.4
3	4892.3	4.4
4	4920.9	0.0
5	4913.9	0.0

The two systems should be interfaced for nonlinear response optimization. The interface procedure is programmed by the C language [27]. To evaluate the equivalent loads in Eqs. (2) and (5), we need the linear stiffness matrix and the nonlinear response. They are generated by ABAQUS and obtained by reading the output files of ABAQUS. The calculated equivalent loads are used as input to GENESIS; therefore, the loads are written on the input file for GENESIS. The iterative process is controlled based on the convergence criteria. These capabilities are coded and the entire process automatically proceeds.

V. Discussion

A. Linear Response Optimization

Linear response optimization is performed under all loading conditions. The results of linear response optimization are used as the initial design of nonlinear response optimization. The results from linear response optimization are shown in Table 3 and Fig. 10. As expected, the maximum stress and displacement occurs by the gust loading condition. After the linear optimization, all the stress constraints are satisfied. Mass is increased by 37.1%. The total number of iterations is five. GENESIS 7.0 is used for linear response structural optimization of the joined wing [26]. As mentioned earlier, the total number of design variables is 2559 and the stresses of all elements except for the edge part are used as constraints. The total CPU time for the linear response structural optimization is 36 h using the HP-UX Itanium II [28].

B. Nonlinear Response Optimization Using the Equivalent Loads Method

Nonlinear response optimization is performed using equivalent loads for the gust loading conditions. In the previous linear response optimization, the 11 loading conditions are used. Only two loading conditions (load cases 8 and 9 in Table 2) are used for the nonlinear response optimization of a joined wing because the gust loading conditions are the most critical. As mentioned in Table 2, the nine loading conditions except for the two gust loading conditions generate relatively small stress responses. Moreover, nonlinear analysis is much more difficult and expensive than linear analysis. Therefore, only two loading conditions are used in nonlinear response optimization and equivalent loads for those two loading conditions are used. As mentioned earlier, the optimum design of linear response optimization is used as the initial design of nonlinear response optimization. Actually, we do not know which initial design is appropriate for nonlinear response optimization. The initial design is not very important if the process converges. Therefore, the initial design is determined to see how the design process of nonlinear response optimization proceeds from the optimum design of linear response optimization.

The results from nonlinear response optimization are shown in Table 4 and Fig. 11. The percent violation of the constraints is illustrated by a log scale. The objective function value is slightly changed after the fourth cycle. The convergence criterion is that the rate of design variable change is less than 1%. The convergence condition is satisfied at the 44th cycle.

When nonlinear analysis considering geometric nonlinearity is performed by the optimum of linear response optimization, the stress constraints are violated up to 1369.3%. This shows that linear optimization is not sufficient for the design of the joined wing with highly geometric nonlinearity. After nonlinear response optimization, all the stress constraints are satisfied. The maximum stress of the optimum design is 179.01 MPa and the wing-tip displacement is 4.468 m. Mass is increased by 60.93%. The total number of cycles is 44. This means that only 44 nonlinear analyses are performed for nonlinear response optimization with several thousand design variables. ABAQUS 6.5 and GENESIS 7.0 are used for nonlinear analysis and linear response structural optimization of the joined wing, respectively [25,26]. The total CPU time for nonlinear response structural optimization is 358 h using the HP-UX Itanium II [28].

C. Nonlinear Response Optimization Using the Fully Stressed Design Method

Nonlinear response optimization is performed using the fully stressed design method for the gust loading conditions. As mentioned earlier, FSD is a non-gradient-based algorithm that is used

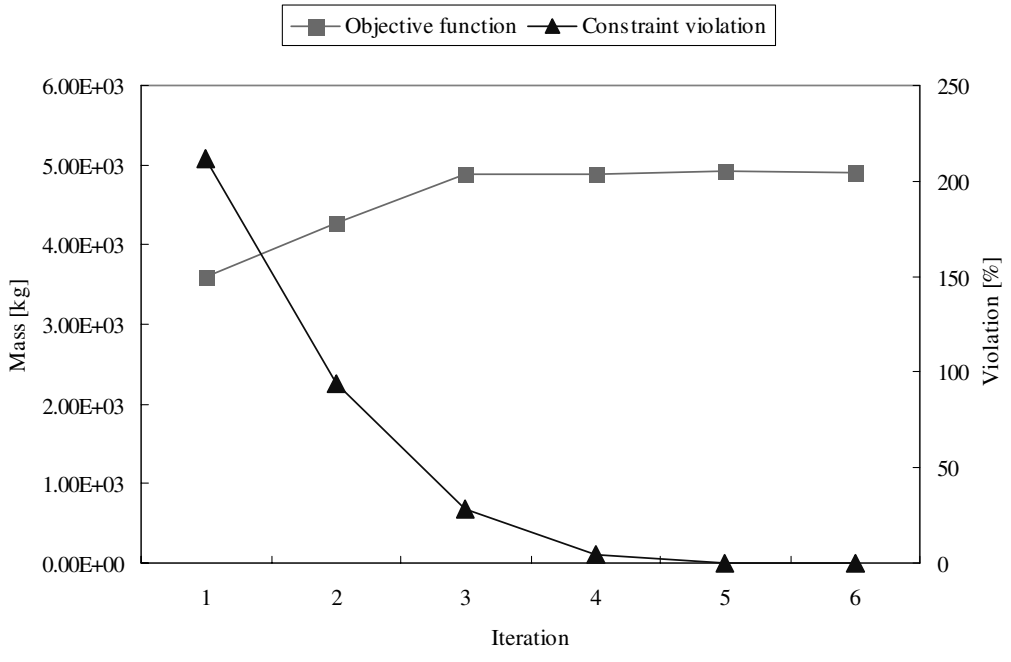

Fig. 10 History of linear response optimization.

Table 4 Results of nonlinear response optimization

Iteration no.	Optimum value, kg	Constraint violation, %
0	4913.9	1369.3
1	13,385.0	35.5
2	6303.9	60.0
3	5853.9	47.4
4	5841.7	41.0
...	...	...
41	5769.0	0.5
42	5768.9	0.5
43	5768.6	0.0
44	5768.5	0.0

for resizing element thicknesses or areas so as to produce a design that satisfies the allowable stress. FSD provides a rapid means of performing initial sizing of aerospace vehicles and allows for the design of a virtually unlimited number of element sizes. Thickness or area can be used as design variables. The FSD method is efficient for designing structures subject only to stress constraints. It is noted that the solution of FSD is not as relatively exact as that of the gradient-based optimization method [18,21].

The concept of FSD is very simple. The design is updated as follows:

$$t^i_{\text{new}} = \left(\frac{\sigma^i}{\sigma_{\text{allowable}}}\right)^{\alpha} t^i_{\text{old}} \quad (i = 1, \ldots, m) \tag{10}$$

where t^i_{new} and t^i_{old} are the new design value and the old design value of the ith element, respectively; m is the number of the design variables; σ^i is von Mises stress of the ith element; $\sigma_{\text{allowable}}$ is the allowable stress value; and α is the relaxation parameter, which can be selected within the range from 0.0 to 1.0.

The optimum design of linear response optimization is used as the initial design. The results from nonlinear response optimization are shown in Table 5 and Fig. 12. The percent violation of the constraint is illustrated by the log scale. The design values are slightly changed after iteration 15. The convergence criterion is that the rate of the design variable is smaller than 1%. The convergence condition is satisfied at the 28th iteration.

When nonlinear analysis considering geometric nonlinearity is performed by the optimum of FSD, the stress constraints are violated up to 2.64%. The maximum stress is 183 MPa on element 1263, which is located at the root of the forewing bottom skin. The final thickness of the element 1263 is 5 cm, which is the upper bound. Therefore, it is difficult to reduce the maximum stress because the thickness of that element cannot be increased further. Other elements satisfy the stress constraints. Mass is increased by 69.78%.

ABAQUS 6.5 [25] is used for nonlinear analysis. All processes for the FSD are coded by the C + + program. The total CPU time for nonlinear response structural optimization is 5 h using the HP-UX Itanium II [28].

D. Discussion

When nonlinear analysis is performed, the optimum design from linear response optimization violates the stress constraints. It has been shown through linear and nonlinear analyses that highly geometric nonlinearity is involved in the joined wing. As illustrated in Figs. 7–9, the difference of the wing-tip displacement is quite large between linear analysis and nonlinear analysis. The difference of the maximum value and distribution of stress is also fairly large.

After linear response optimization, the contour of optimum thickness is illustrated in Fig. 13. The thickness of the aft wing is large in the leading-edge part of the top skin and the trailing-edge part of the bottom skin. The stress contour of the optimum design is illustrated in Fig. 14. The critical stress occurs at the aft-wing part as well as the forewing part.

The contour of the optimum thickness of nonlinear response optimization is illustrated in Fig. 15. The thickness of the aft wing is quite large in the leading-edge part of the top skin and the trailing-edge part of the bottom skin. This result is similar to that of linear response optimization. However, the region of large thickness is larger than that of linear response optimization.

The contour of the optimum thickness of nonlinear response optimization using FSD is illustrated in Fig. 16. The thickness of the aft wing is quite large in the leading-edge part of the top skin and the trailing-edge part of the bottom skin. The thickness of the middle position in the top skin of the aft wing is large. On the other hand, the thickness of the root position in the top skin of the aft wing is large in the result of ELs. In addition, the thickness of the leading-edge spar in the aft-wing root is 2.19 cm in the FSD result. However, that of the ELs result is large, up to 2 times as 5.63 cm.

On the whole, the thickness of nonlinear response optimization is larger than that of linear response optimization. In the two optimizations, the maximum stress occurs at the aft wing. Tip-wing elements

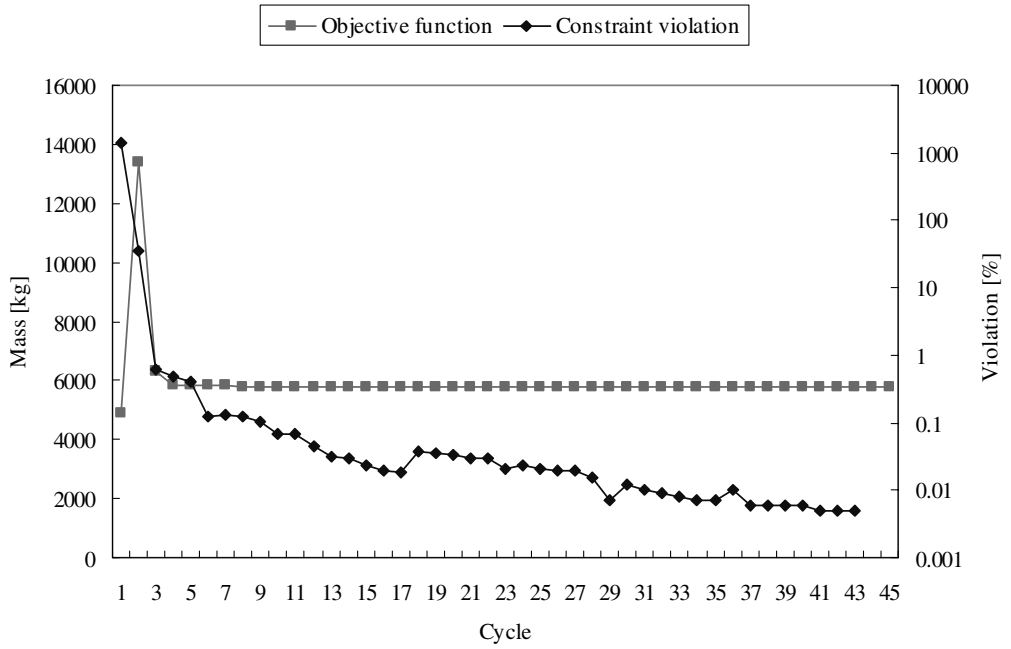

Fig. 11 History of nonlinear response optimization.

Table 5 Results of nonlinear response optimization

Iteration no.	Optimum value, kg	Constraint violation, %
0	4913.9	1369.3
1	6063.5	35.5
2	6068.9	60.0
3	6072.8	47.4
4	6075.6	41.0
...	...	...
25	6084.2	2.6
26	6084.2	2.6
27	6084.3	2.6
28	6084.3	2.6

are thin, and the aft-wing elements have the maximum thickness. In linear response optimization, the trailing-edge spar at the middle position of the aft wing has the maximum thickness. On the other hand, the leading- and trailing-edge spars at the middle position of the aft wing have the large thickness in nonlinear response optimization. The results of linear and nonlinear analyses are fairly different because the direction and the magnitude of the loads are changed according to the deformation of the structure in geometric nonlinear analysis. The optimization results are different accordingly. Therefore, nonlinear response structural optimization is needed when a structure has high nonlinearity. Figures 17 and 18 illustrate the deformation and stress contour of the optimum design of nonlinear response optimization, respectively. As illustrated in Fig. 18, the maximum stress is reduced to the allowable stress 179 MPa. On the other hand, the region of high stress is expanded.

The distribution of optimum thickness from FSD is similar to that of ELs. However, when the nonlinear analysis is performed by the optimum designs of those methods, the stress contour is different, especially in the rib and the bottom skin of the forewing, as shown in Fig. 19. It is noted that the CPU time for nonlinear response optimization is very different between FSD and ELs. The number of nonlinear analyses in FSD is 28 and that of ELs is 44. Although the difference of the number of nonlinear analyses is only 16, the CPU time for ELs is 358 h and that of FSD is 5 h. The reason is that the linear response optimization is needed for the equivalent loads method. The CPU time for linear response optimization is large because this problem has several thousand design variables.

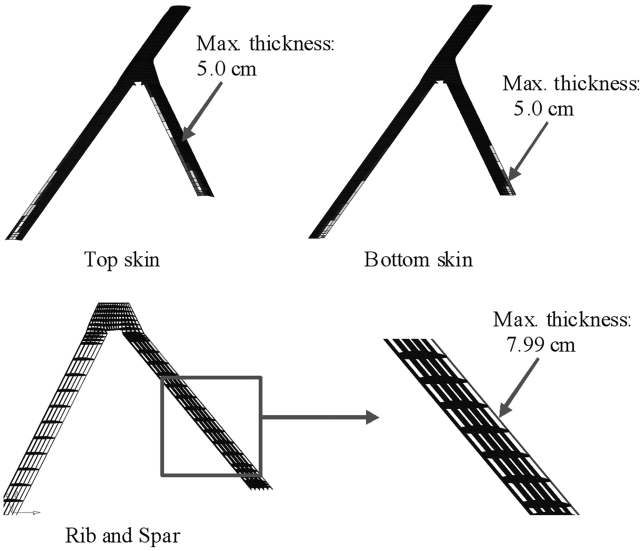

Fig. 13 Thickness contour of the linear response optimization result.

A fully stressed design does not need calculation of sensitivity information. Therefore, the fully stressed design method is efficient for the rapid resizing of a structure. However, this method may not provide an exact solution. On the other hand, the equivalent loads method provides an exact solution. In this research, the optimum mass from FSD is larger by 5.4% than that of ELs. Actually, the equivalent loads method is most efficient for extraction of the exact optimum point. If the problem has high nonlinearity, we can use both methods for the nonlinear response optimization. First, the FSD method is used for nonlinear response optimization. Second, the ELs method is used with the optimum design of the FSD method as an initial design. This process may be more efficient from the viewpoint of saving time and an accurate solution. It should be remembered that we cannot use the FSD method when there are constraints that include global properties of the structure.

Buckling analysis is performed for the optimized design of nonlinear response optimization using ELs. The negative buckling mode occurs in several loading conditions. This means that buckling

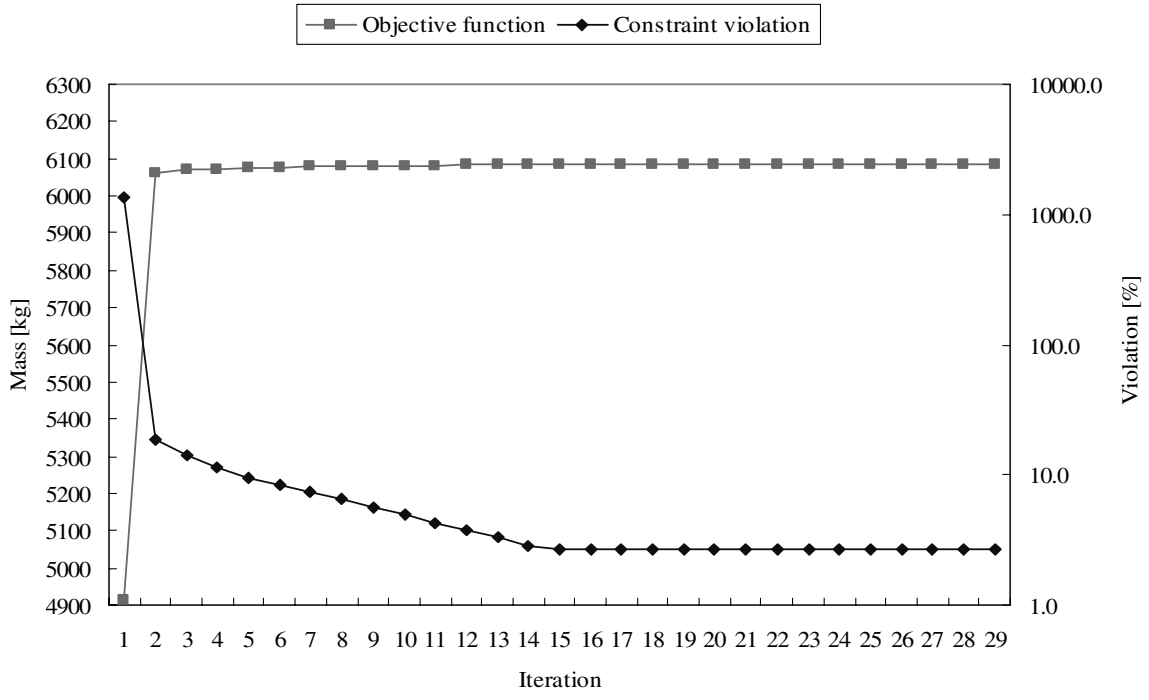

Fig. 12 History of nonlinear response optimization.

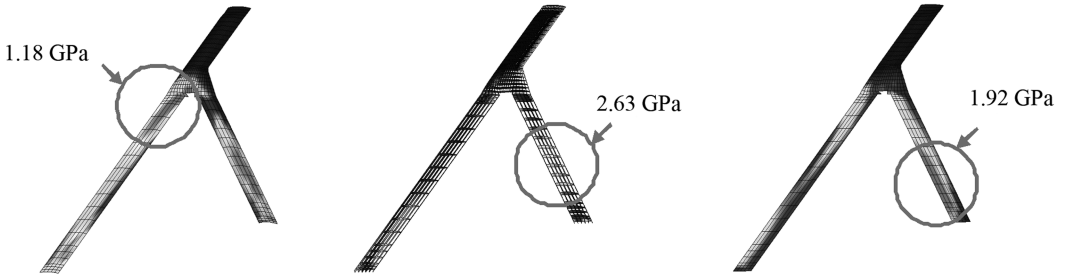

a) Topskin **b) Rib and spar** **c) Bottom skin**

Fig. 14 Stress contours from nonlinear analysis of the linear optimization design.

occurs when the load is reversed. The negative buckling mode is neglected in this discussion. The most critical buckling rate for the taxi crater impact loading condition is 151%. The critical buckling rates for the maneuver and cruise-speed gust loading conditions are 210 and 187%, respectively. The buckling rate of other loading conditions is 416% or higher. The critical buckling mode for the cruise-speed gust loading condition is illustrated in Fig. 20. It is noted that the optimization process does not consider the buckling constraint. However, the buckling constraint is satisfied by the optimized design. In the future, we need to include the buckling constraint.

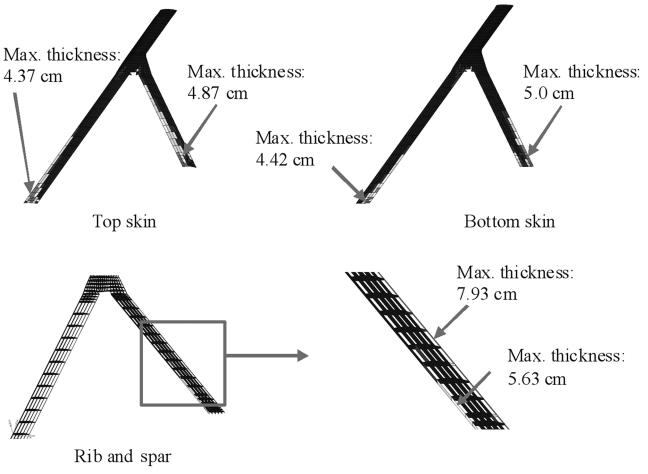

Fig. 15 Thickness contour of nonlinear response optimization result using ELs.

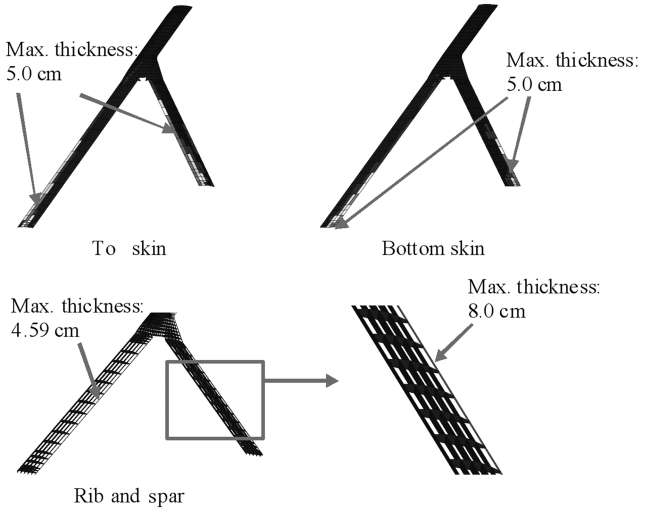

Fig. 16 Thickness contour of nonlinear response optimization result using FSD.

VI. Conclusions

The joined wing that has a longer range and loiter than a conventional wing is investigated from the viewpoint of weight reduction. The joined-wing configuration exhibits large geometric nonlinearity under critical gust load conditions. Moreover, the gust load is the most important in design. Thus, nonlinear analysis under the gust loading condition is required for the design of the joined wing.

The joined-wing structure is optimized. The structure has many design variables. When a design problem is large, nonlinear response structural optimization is very difficult because a large amount of effort is required to calculate the sensitivity information. The equivalent loads method is used as a gradient-based optimization method. The equivalent loads method can be applied to large-scale problems such as a problem with several thousand design variables and constraints, because this method is a very efficient method in that the nonlinear response sensitivity is not required. Equivalent loads are defined as the loads for linear analysis, which generate the same response field as that of nonlinear analysis. A gradient-based optimization method for linear response optimization is used in an iterative manner.

The optimum design considering geometric nonlinearity of the joined wing satisfies all the stress constraints. Although the optimization process does not consider the buckling constraint, the buckling property is improved. The results from nonlinear response optimization and linear response optimization are compared. It is presented that the optimum design from linear response optimization may not be safe for a highly nonlinear problem. The fully stressed design method is used for nonlinear response optimization of the same problem. The results of a fully stressed design and the equivalent loads method are compared. The solution of the equivalent loads method is better than that of a fully stressed design, though FSD provide a rapid means of performing initial sizing of the joined wing.

In the future, nonlinear transient response optimization of the joined wing will be performed using equivalent static loads. The

Fig. 17 Deformation from nonlinear analysis of the optimum design using ELs.

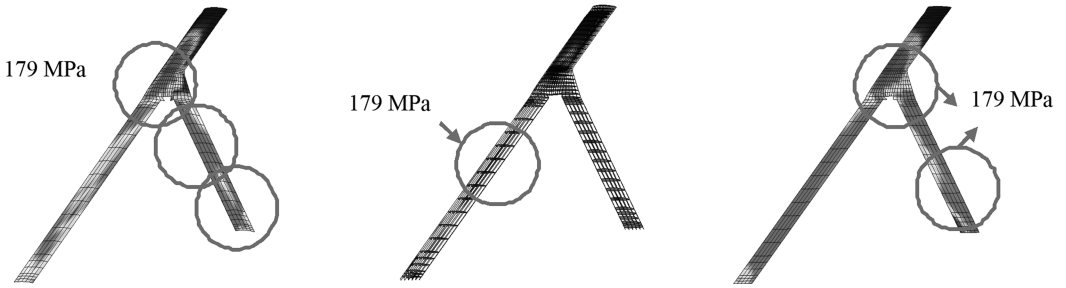

a) Topskin **b) Rib and spar** **c) Bottom skin**

Fig. 18 Stress contours from nonlinear analysis of the optimum design using ELs.

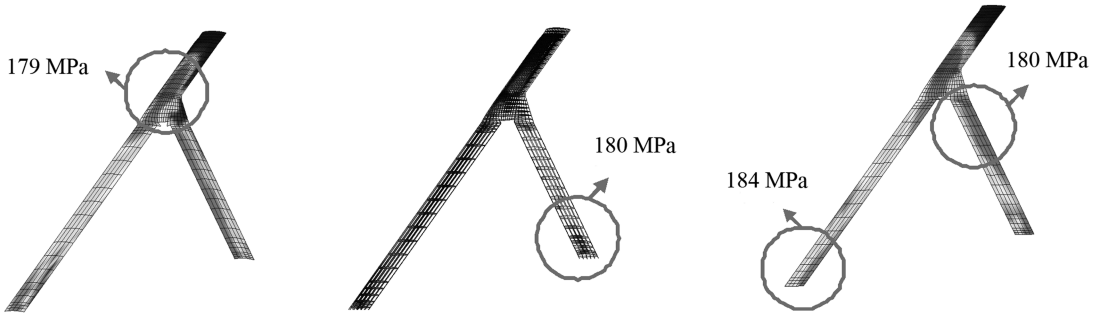

a) Topskin **b) Rib and spar** **c) Bottom skin**

Fig. 19 Stress contours from nonlinear analysis of the optimum design using FSD.

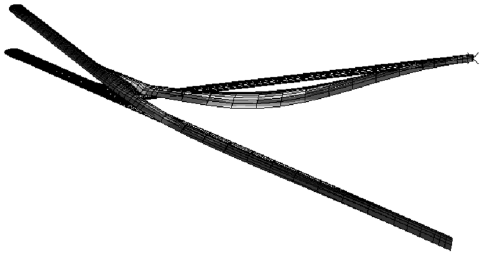

Fig. 20 Critical buckling mode for the cruise-speed gust loading condition.

nonlinear effect as well as the dynamic effect will be considered. Also, the buckling constraints will be considered.

Acknowledgments

This work was supported by the Korea Science and Engineering Foundation grant funded by the Korean government (R01-2008-000-10012-0) and the U.S. Air Force (AOARD-06-4013). The authors are thankful to MiSun Park for her correction of the manuscript.

References

[1] Wolkovich, J., "The Joined Wing: An Overview," *Journal of Aircraft*, Vol. 23, No. 3, 1986, pp. 161–178. doi:10.2514/3.45285

[2] Miura, H., Shyu, A. T., and Wolkovich, J., "Parametric Weight Evaluation of Joined Wings by Structural Optimization," *Journal of Aircraft*, Vol. 25, No. 12, 1988, pp. 1142–1149. doi:10.2514/3.45714

[3] Gallman, J. W., and Kroo, I. M., "Structural Optimization of Joined Wing Synthesis," *Journal of Aircraft*, Vol. 33, No. 1, 1996, pp. 214–223. doi:10.2514/3.46924

[4] Blair, M., Canfield, R. A., and Roberts, R. W., "Joined Wing Aeroelastic Design with Geometric Nonlinearity," *Journal of Aircraft*, Vol. 42, No. 4, 2005, pp. 832–848. doi:10.2514/1.2199

[5] Blair, M., and Canfield, R. A., "A Joined Wing Structural Weight Modeling Study," *AIAA/ASME/ASCE/AHS/ASC Structures, Structural Dynamics, and Materials Conference*, AIAA, Reston, VA, 2002. pp. 1068–1078.

[6] Roberts, R. W., Canfield, R. A., and Blair, M., "Sensor-Craft Structural Optimization and Analytical Certification," *AIAA/ASME/ASCE/AHS/ASC Structures, Structural Dynamics, and Materials Conference*, AIAA, Reston, VA, 2003, pp. 539–548.

[7] Rasmussen, C. C., Canfield, R. A., and Blair, M., "Joined Wing Sensor-Craft Configuration Design," *Journal of Aircraft*, Vol. 43, No. 5, 2006, pp. 1470–1478. doi:10.2514/1.21951

[8] Rasmussen, C. C., Canfield, R. A., and Blair, M., "Optimization Process for Configuration of Flexible Joined Wing," *AIAA/ISSMO Multidisciplinary Analysis and Optimization Conference*, AIAA, Reston, VA, 2004, pp. 1–.

[9] Lee, H. A., Kim, Y. I., Park, G. J., Kolonay, R. M., Blair, M., and Canfield, R. A., "Structural Optimization of a Joined Wing Using Equivalent Static Loads," *Journal of Aircraft*, Vol. 44, No. 4, 2007, pp. 1302–1308. doi:10.2514/1.26869

[10] Cook, R. D., Malkus, D. S., Plesha, M. E., and Witt, R. J., *Concepts and Applications of Finite Element Analysis*, 4th ed., Wiley, New York, 2001.

[11] Hoblit, F. M., *Gust Loads on Aircraft: Concepts and Applications*, AIAA, Washington, D.C., 1988, Chaps. 2, 3.

[12] Katz, J., and Plotkin, A., *Low-Speed Aerodynamics*, McGraw–Hill, New York, 1991.

[13] Reddy, J. N., *An Introduction to Nonlinear Finite Element Analysis*, Oxford Univ. Press, New York, 2004.

[14] Bathe, K. J., *Finite Element Procedures*, Prentice–Hall, Upper Saddle River, NJ, 1996.

[15] Ryu, Y. S., Haririan, M., Wu, C. C., and Arora, J. S., "Structural Design Sensitivity Analysis of Nonlinear Response," *Computers and Structures*, Vol. 21, Nos. 1–2, 1985, pp. 245–255. doi:10.1016/0045-7949(85)90247-0

[16] Wu, C. C., and Arora, J. S., "Design Sensitivity Analysis and Optimization of Nonlinear Structural Response Using Incremental Procedure," *AIAA Journal*, Vol. 25, No. 8, 1987, pp. 1118–1125. doi:10.2514/3.9752

[17] Suleman, A., and Sedaghati, R., "Benchmark Case Studies in Optimization of Geometric Nonlinear Structures," *Structural and Multidisciplinary Optimization*, Vol. 30, No. 4, Oct. 2005, pp. 273–296.

[18] Haftka, R. T., and Gürdal, Z., *Elements of Structural Optimization*, Kluwer Academic, Norwell, MA, 1992.
[19] Arora, J. S., *Introduction to Optimum Design*, McGraw–Hill, New York, 2001.
[20] Park, G. J., *Analytical Methods in Design Practice*, Springer–Verlag, Berlin, 2007.
[21] *MSC.Nastran 2004 Reference Manual*, MSC Software Corp., Santa Ana, CA, 2004.
[22] Shin, M. K., Park, K. J., and Park, G. J., "Optimization of Structures with Nonlinear Behavior Using Equivalent Loads," *Computer Methods in Applied Mechanics and Engineering*, Vol. 196, Nos. 4–6, 2007, pp. 1154–1167. doi:10.1016/j.cma.2006.09.001
[23] Kim, Y. I., Lee, H. A., and Park, G. J., "Case Studies of Nonlinear Response Structural Optimization Using Equivalent Loads," *The 4th China-Japan-Korea Joint Symposium on Optimization of Structural and Mechanical Systems (CJKOSM4)*, 2006, pp. 83–88.
[24] Park, K. J., and Park, G. J., "Structural Optimization of Truss with Nonlinear Response Using Equivalent Linear Loads," *Transactions of the Korean Society of Mechanical Engineers (A)*, Vol. 28, No. 4, 2004, pp. 467–474 (in Korean).
[25] ABAQUS, Software Package, Ver. 6.5, Hibbitt, Karlsson and Sorensen, Inc., Pawtucket, RI, 2004.
[26] GENESIS, Software Package, Ver. 7.0, Vanderplaats Research and Development, Inc., Colorado Springs, CO, 2001.
[27] C++: *The Core Language*, 1st ed., O'Reilly & Associates, Indianapolis, IN, 1995.
[28] *HP TestDrive* [online database], http://www.testdrive.hp.com/current.shtml [retrieved 20 Mar. 2007].

A. Messac
Associate Editor